Upregulation of DEK Expression in Uterine Myomas and Cervical Cancer as a Potential Prognostic Factor

Anastasia Tsigkou[1*], Amelia Janiak[1], Peng Cheng Tan MS[1], Ferdinand Kappes[1], Felice Petraglia[3], Chiara Donati[3], Xinyue Liu[1], Renata Koviazina[1], Fangrong Shen[2]

[1]Division of Natural and Applied Sciences, Duke Kunshan University, Kunshan, China; [2]No 1 Affiliated Hospital Suzhou University, Department of Gynecology, Suzhou, China; [3]Obstetrics and Gynecology, Department of Experimental and Clinical Biomedical Sciences, Obstetrics and Gynecology, University of Florence, Florence, Italy

ABSTRACT

Background: Gynecological tumors, including uterine myomas and cervical cancer, significantly affect women's health worldwide. Despite advances in diagnostic tools, reliable biomarkers remain limited. DEK, a protooncogene involved in chromatin remodeling, DNA repair, and transcription regulation, has shown potential as a prognostic marker in several malignancies. This study investigates DEK expression in uterine myomas and cervical cancer tissues compared to normal uterine tissues.

Methods: Tissue samples from Chinese female patients undergoing surgery for uterine myomas or cervical cancer were collected. DEK mRNA levels were investigated using quantitative real-time polymerase chain reaction (qRT-PCR), and DEK protein levels were analyzed using immunohistochemistry and Western blotting. Statistical analyses, including ANOVA, Tukey's HSD, Kruskal-Wallis H, and Mann-Whitney U tests, were performed to assess differences in expression among tissue types.

Results: Immunohistochemical analysis revealed significantly elevated DEK protein expression in cervical cancer tissues, moderate expression in uterine myomas, and minimal expression in normal uterine tissues. Western blotting confirmed these findings, showing statistically significant differences in DEK protein levels between normal and pathological tissues. However, qRT-PCR results indicated no statistically significant differences in DEK mRNA expression across tissue types.

Conclusion: Elevated DEK protein expression in cervical cancer and uterine myoma tissues suggests its involvement in both tumor development and suppression, making it a promising biomarker for early detection in gynecological tumors. Further research is necessary to elucidate DEK's mechanisms in gynecological tumorigenesis and its potential as an early biomarker, addressing a critical need in women's health.

Keywords: DEK oncogene; Uterine myoma; Cervical cancer; Gynecological cancers; Fertility

Citation: Anastasia Tsigkou, Amelia Janiak, PengCheng Tan MS, Ferdinand Kappes, Felice Petraglia, Chiara Donati, Xinyue Liu, Renata Koviazina, and Fangrong Shen (2025) Upregulation of DEK Expression in Uterine Myomas and Cervical Cancer as a Potential Prognostic Factor, Gynecol. Obstet. 15(1)

INTRODUCTION

Tumors of the female reproductive system are very common, with uterine myomas being the most frequent benign tumor and cervical cancer the most common malignancy [1, 2]. Uterine myomas, or fibroids, originate from the overgrowth of smooth muscle and connective tissue in the uterus, affecting approximately 50% of women of reproductive age and often causing complications such as pelvisalgia, menorrhagia, and fertility issues. By comparison, cervical carcinoma arises from the cervix's cellular structure and poses a significant health risk without timely diagnosis and intervention [1-6].

Current screening methods for cervical cancer and fibroids employ tools such as transvaginal ultrasound, pelvic exams, MRI, and Pap smears. For cervical cancer, Pap smears remain the primary test recommended every three years for women aged 21 years–65 years [7]. Combined Pap smears and HPV testing, particularly for high-risk types like HPV-16 and HPV-18, improve sensitivity up to 96% but still have limitations, with Pap smears showing only 50% sensitivity on average and false negatives at 35.5% [8-10]. For uterine fibroids, transvaginal ultrasound and MRI are optimal for assessing size, location, and structure, though ultrasound's effectiveness can be limited by operator dependency and patient factors, while MRI offers superior resolution but at higher cost and reduced accessibility [11, 12]. Integrating biomarkers such as p16/Ki-67 dual staining for cervical cancer and genetic markers like MED12, HMGA2, and FH for fibroids shows promise for improving diagnostic accuracy and advancing personalized care [13-15]. However, the addition of more genetic and protein markers is needed to further improve diagnostic precision and patient outcomes. Given an urgent need for improved screening methods and the rising prevalence of gynecological tumors with profound impact on quality of life, including physical, emotional, and psychological well-being, current research is increasingly focused on novel agents that target the DNA Damage Response (DDR) [16, 17]. DDR comprises a set of signaling pathways for the detection and repair of DNA damage, including machinery mediating DNA repair, cell cycle regulation, replication stress responses and apoptosis [18]. Indeed, the progression of cervical cancer is associated with an increased genetic instability, which is primarily caused by the DNA damage and breakage [19]. Enhanced comprehension of DDR processes offers potential for cancer treatment by elucidating cellular and molecular signaling mediators pivotal in tumor development and progression. The chromatin-associated oncogene DEK, a promising yet underexplored biomarker, is encoded by the DEK gene located at chromosome 6p22.3 and produces a 43 kDa nuclear protein predominantly expressed in malignant and actively dividing cells [20, 21]. Initially identified for its role in chromatin organization and gene regulation, DEK has been implicated in essential processes including DNA damage repair, RNA transcriptional regulation, mRNA splicing, and DNA replication. Elevated DEK levels have been shown to promote proliferation, motility, invasion, and tumorigenesis, with upregulation observed in acute myeloid leukemia, retinoblastoma, glioblastoma, melanoma, and other cancers [22-31]. In CaSki cervical cancer cells, DEK suppression has been linked to cell cycle arrest in the G0/G1 phase, reduced G2/M phase progression, increased apoptosis, and enhanced cell senescence, suggesting its oncogenic role in tumor development [32]. Xu et al. further demonstrated that silencing DEK in cervical cancer inhibits proliferation, migration, and invasion by downregulating Wnt/β-catenin and MMP-9, enhancing GSK-3β activity, and impairing tumorigenicity in a mouse xenograft model, correlating DEK expression with FIGO staging and tumor aggressiveness [33]. The oncogenic role of DEK is part of a broader mechanism wherein the accumulation of genetic damage, including proto-oncogene activation and tumor-suppressor gene inactivation, drives the transformation of healthy cells into malignant ones [34]. Proto-oncogenes like DEK, which regulate cell differentiation and proliferation, can undergo activation through genetic pathways such as amplification, point mutations, transduction, insertional mutagenesis, and chromosomal translocations, resulting in deregulated expression that confers a proliferative advantage to cells [35]. As an oncogene, DEK promotes tumorigenesis by disrupting cell division, impairing DNA repair, inhibiting differentiation and apoptosis, inducing senescence, and cooperating with other oncogenes. Supporting this, Han et al. demonstrated that DEK is critical for serous ovarian cancer cell proliferation, with high expression levels correlating with increased Ki-67 indices, while Privette et al. showed that DEK stimulates cellular proliferation through wnt signaling in Ron receptor-positive breast cancers [36-38]. DEK overexpression, while primarily linked to malignancies, has also been observed in certain benign tumors. DEK knockout mouse models show partial resistance to benign skin papillomas, suggesting its role in early tumorigenesis and growth regulation [39]. In contrast, studies such as Riveiro-Falkenbach et al. report negligible DEK expression in benign lesions, and research on melanocytic lesions reveals low or absent DEK expression in benign nevi and melanoma in situ [40,41]. These conflicting findings highlight the limited understanding of DEK's role in benign tumors, underscoring the need for further investigation into its involvement in early tumorigenic processes. Given DEK's critical role in tumorigenesis and DNA repair, along with the limited research on its function in benign tumors and the need for more accurate diagnostic biomarkers for Pap smears, our study aimed to evaluate DEK expression as a potential prognostic factor in both benign gynecological tumors and malignant gynecological cancers. Through immunohistochemical, Western blot, and quantitative Real Time Polymerase Chain Reaction (qRT-PCR) analyses, we observed significant DEK upregulation in cervical carcinomas, moderate expression in uterine myomas, and negligible expression in normal uterine tissues, with statistically significant differences across these tissues.

MATERIALS AND METHODS

Tissue samples

This pilot study aimed to investigate differences in DEK expression between benign uterine myomas and cervical cancer tissues. Specimens, including myomas, normal myometrial tissues, and cervical cancer samples, were collected according to the guidelines of the Institutional

Review Board of the No. 1 Affiliated Hospital of Suzhou University (Department of Obstetrics and Gynecology, China) and Duke Kunshan University, Kunshan, China. Written informed consent was obtained from all patients prior to surgery.

Sample collection and processing: Between January and June 2023, tissue samples were obtained from ten women with uterine myomas, four with cervical cancer, and three with normal uterine tissues, with each sample originating from a different patient. Uterine myoma and cancer samples were not matched with control samples. Surgeries were conducted to address symptoms such as long-term heavy bleeding, abdominal pain, and dysmenorrhea during the luteal phase. Diagnostic assessments, including transvaginal ultrasound and Pap smears, were performed prior to surgery. Normal tissues were collected from patients with no history of fibroids, endometriosis, or cancer.

Clinical parameters, including patient age, number of leiomyomas, VAS pain index, and menstrual cycle phase (middle to late proliferative), were recorded for the uterine myoma group. None of the patients had received steroid hormone therapy (OAC, IUD, or HRT) for at least three months prior to surgery. Endometrial tissue samples (0.4 g–1.2 g) were scraped from the uterine fundus immediately after surgery, while cone biopsy samples were obtained for cervical cancer cases. In uterine myoma patients, tissue was collected from the opposite side of the uterus to avoid interference from fibroid growth. All tissue specimens were snap-frozen in liquid nitrogen and stored at -80°C for subsequent analysis.

Pathological confirmation and limitations: Pathological examination at the No. 1 Affiliated Hospital confirmed the diagnosis of uterine myomas and cervical cancer, with staging and histological subtyping performed according to the 1988 FIGO criteria. All fibroid and cervical cancer samples were staged at FIGO I–III [42-52]. Due to the small sample size, no a priori power analysis was conducted; instead, all available samples were analyzed as part of this pilot investigation.

Immunohistochemical analysis

Immunohistochemical studies of tissue explants: Immunohistochemical staining for DEK (1:1000, DEK (Abcam, ab26) proteins was performed using formalin-fixed and paraffin-embedded tissue slides, a detection kit (DAKO ChemMate, DAKO, Glostrup, Denmark) and a semi-automated stainer (DAKO TechMate, DAKO, Glostrup, Denmark) according to the specifications of the manufacturer. For antigen retrieval the slides were treated in a PT Link module (DAKO, Glostrup, Denmark) using the EnVision™ FLEX Target Retrieval Solution, Low pH (DAKO, Glostrup, Denmark). Quantification of DEK expression was performed using QuPath image analysis software, which facilitated semi-automated analysis of DAB-positive cells. Two independent observers evaluated the samples, and the optical staining intensity was determined (graded as 0: no staining; 1: weak; 2: moderate; and 3: strong staining) along with the percentage of positive cells (0: no staining; 1: <10%; 2: 11%-50%; 3: 51%-80%; 4: >81% of cells). The IRS score was calculated by multiplying these two values.

Western blot analysis

Protein extraction: Tissues were dissected on ice and transferred to microcentrifuge tubes. For 100 mg of tissue, 400 µL of ice-cold RIPA lysis buffer with PMSF (Beyotime, P0013 B) was added, and the tissue was homogenized using a pestle and a mortar. Additional 600 µL of lysis buffer was added during the homogenization process. The sample was kept on ice and agitated on an orbital shaker for 1.5 hours. Subsequently, the tubes were centrifuged at 4°C. The supernatant containing extracted proteins was collected into a fresh tube and stored at -80°C.

Western blot: Total protein concentration was determined using the Enhanced BCA Protein Assay Kit (Beyotime, China, P0009). The proteins and deionized water were mixed to make sure each sample had the same concentration with a total of 20 µL or 30 µL. 5 µL of 5x SDS-PAGE Loading Buffer (NCM Biotech, WB2001) was then added to each sample, followed by vortex, incubation at 95°C for 5 min and centrifugation at 1,000 g for 10 seconds. Total protein (16 µg per lane) was separated using a SDS-polyacrylamide gel and transferred onto a nitrocellulose membrane. SeeBlue Plus2 Pre-Stained Standard (Invitrogen, Karlsruhe, Germany) was used as a marker. The membranes were incubated with primary anti-DEK (rabbit, 1:2000; Abcam, ab26) and anti-GAPDH (rabbit, 1:1000; Beyotime, AG0122) followed by incubation with the corresponding secondary antibodies (HRP-conjugated goat anti-rabbit IgG, 1:5000, MULTISCIENCE, GAR0072). The bands were visualized by incubating the membrane with ECL solution (TanonTM High-sig ECL Western Blotting Substrate (Biotanon,180-501) and examined in a pre-cooled chemiluminescence imaging system (Bio-Rad Laboratories, CA, USA) according to the manufacturer's instructions. Image analysis was performed with the ImageJ to obtain quantifiable DEK protein expression levels, normalized to the expression of the reference gene (GAPDH).

qRT-PCR analysis

RNA extraction: Tissue samples stored at -80°C were crushed until a fine powder using a mortar and a pestle. Approximately 100 mg powder was recovered from each sample and placed into a new cold microtube. Then, RNA was extracted using the TRIzol reagent (ThermoFisher Scientific, 15596026) protocol provided by the manufacturer, using TRIzol reagent, chloroform (Titan, G75915B) and isopropanol (Titan, G75885B). After RNA extraction, 20 µL of DEPC water (DNase, RNase free) (damas life, G 8010 ml-500 ml) was added to the sample and it was stored at -80°C.

cDNA synthesis: cDNA synthesis was carried out using HiScript II 1st strand cDNA synthesis kit (Vazyme, R211-02). About 500 ng of total RNA were reverse transcribed with 200 U/µl of M-MLV reverse transcriptase (Invitrogen), RNase Out, 150 ng random hexamers and 10 mM dNTPs according to the manufacturer's instructions. RNA was denatured at 65°C for 5 min and subsequently kept on ice for 1 min. After adding the enzyme to the RNA primer mixes, samples were incubated for 10 min at 25°C to allow annealing of the random hexamers. Reverse transcription was performed at

37°C for 50 min followed by inactivation of the reverse transcriptase at 70°C for 15 min.

qRT-PCR: qRT-PCR was utilized in human tissue samples to analyze gene expression levels of two proteins: DEK and GAPDH. Relative quantification of transcription levels was carried out by real-time PCR analyses using the Applied Biosystems 7300 real-time PCR system (Applied Biosystems) and ChamQ universal SYBR qPCR Master Mix kit (Vazyme, Q711-02) according to the manufacturer's instructions. Sequences for primers were found in scientific literature and commercially synthesized by Sangon Biotech (Table 1). The amplification reaction mixture (total volume of 20 μL) contained 2 × ChamQ Universal SYBR qPCR Master Mix, 0.4 μL of forward primer (10 μM), 0.4 μL of reverse primer (10 μM), 2 μL of template cDNA, and DEPC-H2O (added to the final volume). Incubation conditions were: 1) initial denaturation: 95°C/30 sec; 2) cycling reaction: 40 cycles of 95°C/10 sec and 60°C/60 sec; 3) melting curve: 95°C/15 sec, 60°C/60 sec, 95°C/15 sec.

Table 1: Primer sequences for qRT-PCR. Sequences for primers were found in scientific literature and commercially synthesized by Sangon Biotech.

Gene	Primer Sequence
DEK	Forward: 5'-TGGGTCAGTTCAGTGGCTTTCC-3'
DEK	Reverse: 5'-CTCTCCAAATCAAGAACCTCACAG-3'
GAPDH	Forward: 5'-ACAACTTTGGTATCGTGGAAGG-3'
GAPDH	Reverse: 5'-GCCATCACGCCACAGTTTC-3'

Statistical analysis

To determine the statistical significance of DEK protein expression differences among the three tissue types, two statistical tests were utilized to analyze Western blot results. First, one-way ANOVA test was performed to determine if there were any overall significant differences in DEK expression among the groups. Following a significant ANOVA result, post-hoc Tukey's Honest Significant Difference (HSD) test was conducted to identify specific pairwise differences between the groups.

The results of the qRT-PCR were expressed as $2^{-\Delta\Delta Ct}$, which is the fold change in gene expression relative to the control (normal uterine tissue), calculated as the difference between the delta cycle threshold (ΔCt) of the target gene and the ΔCt of the reference gene (GAPDH). To compare gene expression patterns, relative gene expression was graphed in GraphPad Prism 10. Statistical analysis was conducted using Kruskal-Wallis H test and unpaired Mann-Whitney U test. Kruskal-Wallis H test was employed to assess the presence of overall differences in expression among normal uterine tissue, uterine myoma, and cervical carcinoma samples, while unpaired Mann-Whitney U test was used to further examine and identify specific group differences.

RESULTS

Cervical intraepithelial neoplasia of different stages was obtained (cervical intermediate differentiated adenocarcinoma IB1 = 2, cervical low-grade squamous cell carcinoma IIIC1 = 1, cervical low-grade squamous cell carcinoma IB (specific IB123 pathology unknown) = 1). The median age at the time of diagnosis for patients with cervical cancer was 44, with 28-53 age range. The clinicopathological features of uterine myomas are summarized in (Table 2).

Table 2: Clinical characteristics of women with uterine myomas (n=10).

Symptom	Number of Women Experiencing the Symptom	
Menstrual bleeding	10	
Intermenstrual bleeding	10	
Characteristic	Median	Interquartile Range
Age (years)	42	28-53
Dysmenorrhea (VAS)	3	2-4
Intermenstrual pelvic pain (VAS)	3	2-5
Largest myoma diameter (mm)	90	3-90
Uterine volume (cm^2)	126	65-198
Number of myomas	2	1-6
Type	Submucous*	2

	Intramural fibroids**	2
FIGO staging	I	1
	II	1
	III	8

Note: VAS stands for Visual Analog Scale. *submucosal fluid with intramural extension smaller or bigger 50%; ** in contact with the endometrium, but not extending into the uterine cavity or serous surface.

Immunohistochemical analysis

Expression levels of DEK protein in normal uterine, uterine myoma and cervical carcinoma tissue samples were determined via immunohistochemical counterstaining. Representative immunohistochemical images are shown in figure 1A-1E and the IRS scores are presented in Figure 1F.

The data indicates a significant upregulation in DEK protein expression in cervical cancer tissue, with a high final IRS score of 12, indicating strong positive expression. In uterine myoma tissue, DEK expression is present but at a lower level, with a final IRS score of 2, indicating positive expression. Normal tissue shows little to no DEK expression, with a final IRS score of 0.

(A) (B) (C) (D) (E) (F)

(G)
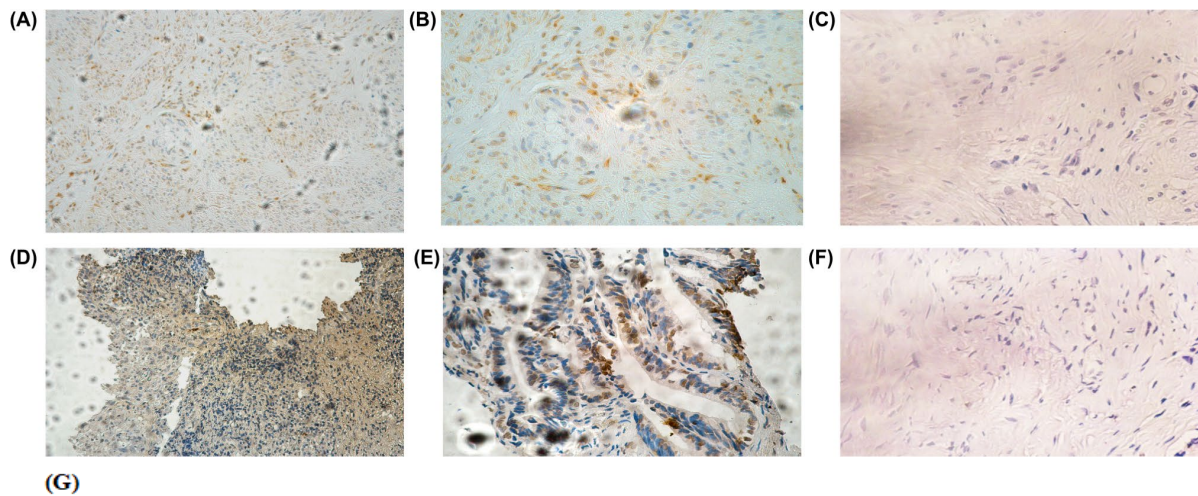
Tissue type	Percentage of Positive Cells	Positive Cells Score	Staining Intensity	Staining Intensity	Final IRS Score	Expression Level
Uterine Myoma	<10%	1	Weak	2	2	+
Cervical Cancer	>81%	4	Strong staining	3	12	++
Normal Uterine Tissue	No staining	0	No staining	0	0	−

Figure 1: Immunohistochemical Staining and Analysis of DEK Expression in Uterine Myomas and Cervical Cancer Tissues.

Note: Immunohistochemical staining for DEK (1 mg/ml, Abcam) was conducted on formalin-fixed, paraffin-embedded tissues using a detection kit (DAKO ChemMate) and a semi-automated stainer (DAKO TechMate) according to the specifications of the manufacturer. (A) Nuclear staining of DEK, uterine myoma (x20). (B) Nuclear staining of DEK, uterine myoma (x40). (C) Negative control for nuclear staining of DEK, uterine myoma (x40). (D) Nuclear staining of DEK, cervical cancer (x20). (E) Nuclear staining of DEK, cervical cancer (x40). (F) Negative control for nuclear staining of DEK, cervical cancer (x40). (G) To quantify DEK expression in uterine myomas and cervical cancer tissues immunohistochemical staining analysis was conducted. The IRS score was calculated by multiplication of the optical staining intensity (0, no staining; 1, weak; 2, moderate; 3, strong staining) and the percentage of the positive stained cells (0, no staining; 1, <10%; 2, 11-50%; 3, 51-80%; 4, >81% of the cells). The expression level of DEK was then categorized into three levels: negative (−), positive (+), and strongly positive (++).

Western blot analysis

Western blotting was used to investigate DEK protein expression levels in normal uterine tissue, uterine myoma tissue and cervical cancer tissue samples. The results were analyzed using a computer program (ImageJ) and were normalized to GAPDH expression.

Figure 2 shows, relative DEK protein expression level is highest in cervical cancer tissue ($\sim$5.7), intermediate in uterine myoma tissue ($\sim$4.0), and lowest in normal uterine tissue ($\sim$1.0). Statistical analysis with ANOVA test showed a significant difference in DEK expression among the tissue types (p=0.0038). Post-hoc analysis with Tukey's HSD test confirmed significant differences between normal and uterine myoma tissues (p<0.05) and between normal and cervical

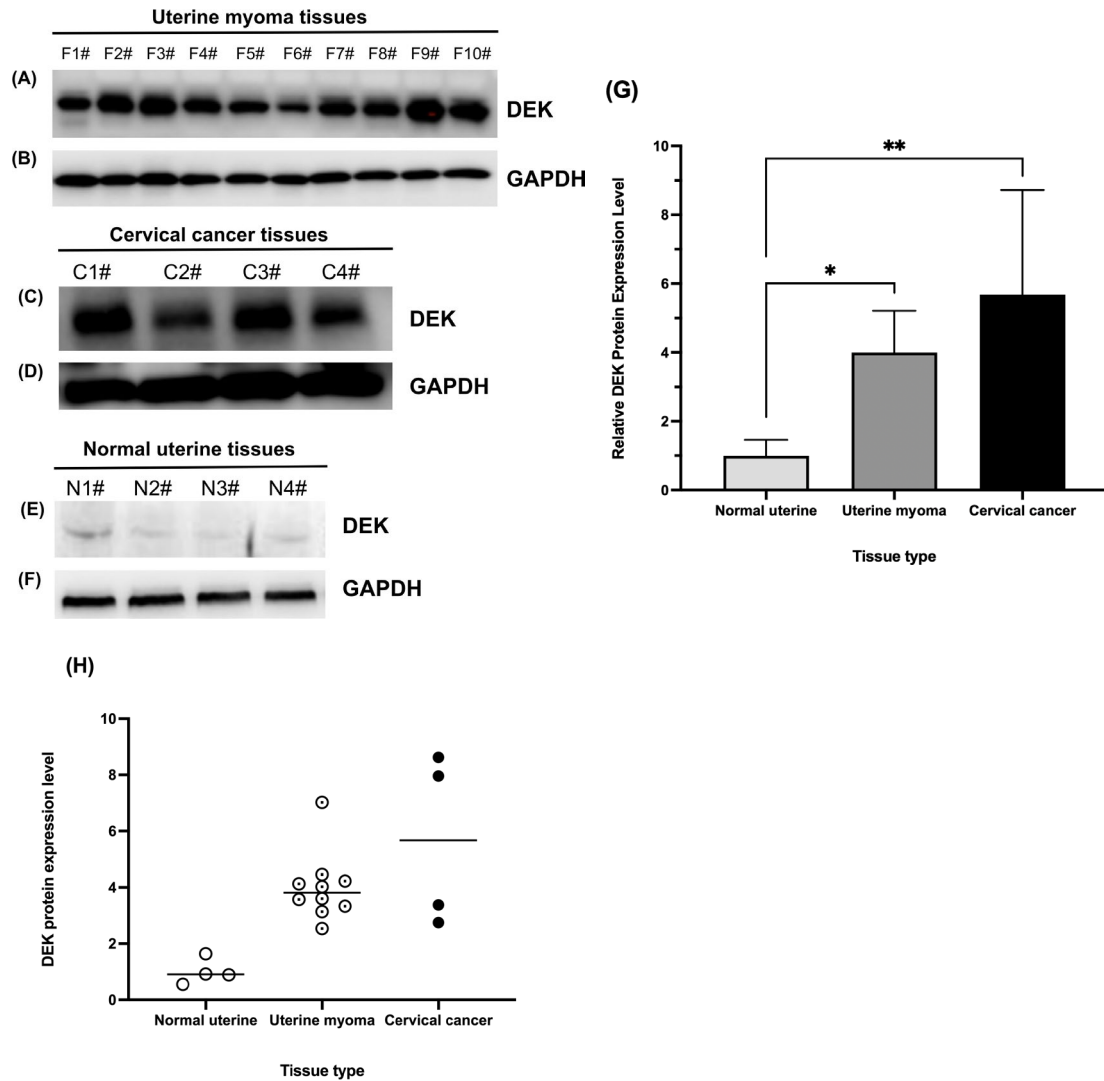cancer tissues (p<0.01), but not between uterine myoma and

cervical cancer tissues (p>0.23).

Figure 2: Relative DEK Protein Expression in Normal Uterine Tissue, Uterine Myoma Tissue, and Cervical Cancer Tissue.

Note: Western blot analysis of protein expression: (A) DEK in uterine myoma (F1#-F10#), (B) GAPDH in uterine myoma (F1#-F10#), (C) DEK in cervical cancer (C1#-C4#), (D) GAPDH in cervical cancer (C1#-C4#), (E) DEK in normal uterine (N1#-N4#), (F) GAPDH in normal uterine (N1#-N4#). Antibodies: DEK (rabbit, 1:2000, Abcam), GAPDH (rabbit, 1:1000, Beyotime). (G) Quantification of DEK and GAPDH protein levels from the Western blots in panels A-F using ImageJ gel analysis program. Data are presented as mean and standard deviation (error bars). Statistical analysis was performed using one-way ANOVA (p = 0.0038) and Tukey's HSD test for pairwise comparisons: normal vs. uterine myoma (p < 0.05), normal vs. cervical cancer (p < 0.01), uterine myoma vs. cervical cancer tissue (p > 0.23). *, p < 0.05; **, p < 0.01. (H) Relative DEK protein expression within individual biological samples.

qRT-PCR

To analyze DEK expression at the transcriptional level, mRNA was extracted from samples of cervical cancer, uterine myomas and normal uterine tissue, transcribed into cDNA, and followed by qRT-PCR analysis.

Figure 3 demonstrates that in normal uterine tissue, relative DEK mRNA expression is relatively low, with an average at 1.031. The uterine myoma tissue exhibits higher relative expression, with an average close to 1.085, indicating an upregulation in this tissue type. In cervical cancer tissue, the

relative DEK mRNA expression is similar to that of uterine myoma tissue, averaging around 1.091. These results suggest that similarly to protein levels, DEK mRNA is upregulated in uterine myoma tissue and cervical cancer tissues, which show similar expression levels. Statistical analysis, however, demonstrated that there are no statistically significant differences in DEK expression levels among the three tissue types (Kruskal-Wallis H (p=0.503); unpaired Mann-Whitney U test: normal vs. uterine myoma tissues (p=0.349), normal uterine vs. cervical cancer tissues (p=0.571), uterine myoma vs. cervical cancer tissues (p=0.566)).
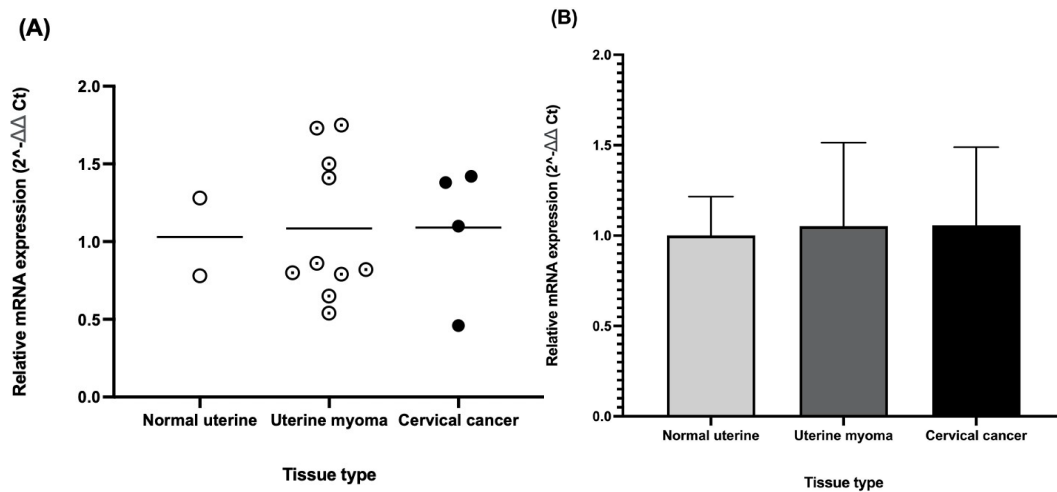
Figure 3: Relative DEK mRNA expression levels in normal uterine tissue, uterine myoma tissue, and cervical cancer tissue.

Note: Relative quantification was performed using the Applied Biosystems 7300 real-time PCR system and ChamQ Universal SYBR qPCR Master Mix. Primers for DEK and GAPDH were sourced from literature and synthesized by Sangon Biotech. (A) Relative DEK mRNA expression ($2^{\wedge}$-$\Delta\Delta$Ct). (B) Mean relative DEK mRNA expression ($2^{\wedge}$-$\Delta\Delta$Ct) with standard deviations (error bars). No statistically significant differences in DEK expression levels among the three tissue types were found.

DISCUSSION

Our pilot study demonstrates varying DEK expression in normal uterine tissues, uterine myomas, and cervical cancer tissues, suggesting that DEK plays distinct, context-dependent roles in gynecological pathology. Immunohistochemical analysis revealed significant DEK upregulation in cervical cancer tissues, moderate expression in uterine myomas, and negligible levels in normal uterine tissues. Western blot analysis, normalized to GAPDH, confirmed this trend, showing the highest DEK protein expression in cervical cancer, followed by uterine myomas, and the lowest in normal tissues. qRT-PCR analysis further demonstrated elevated DEK mRNA levels in uterine myomas and cervical cancer compared to normal tissues, consistent with the protein expression patterns. Statistical analysis of Western blot data using one-way ANOVA and Tukey's HSD post-hoc test identified significant differences in DEK protein expression across groups, while no significant differences in mRNA expression were observed, likely due to the limited sample size of this pilot study.

DEK's marked upregulation in cervical cancer tissues supports its role as a potential oncogene, aligning with prior evidence demonstrating DEK's involvement in promoting cell proliferation, motility, invasion, and tumorigenesis [26, 28, 29, 33, 44]. In reproductive system cancers such as breast cancer, DEK overexpression has been shown to activate the Wnt/β-catenin pathway, leading to increased β-catenin levels and upregulation of downstream targets like cyclin D1 and c-Myc, enhancing tumor proliferation and invasiveness [45]. Additionally, DEK can promote angiogenesis and metastasis through activation of the PI3K/AKT/mTOR signaling cascade, further underscoring its critical role in tumor progression and its therapeutic potential in gynecological malignancies [53-56]. Conversely, the intermediate DEK expression observed in uterine myomas suggests a context-dependent tumor-suppressive role. This may represent a compensatory mechanism to regulate cellular proliferation and preserve genomic stability, thereby counteracting the

potential for malignant transformation. DEK has been shown to mitigate replication stress-induced DNA damage by stabilizing stalled replication forks, similar to DNA repair proteins such as FANCD2 and RAD51, which prevent double-strand break formation and maintain replication fork integrity [22, 46, 47]. The elevated DEK levels in myomas may thus reflect a protective response to prevent genomic instability and maintain tissue homeostasis in a benign context. In contrast, the negligible DEK expression in normal uterine tissues aligns with its preferential expression in rapidly proliferating or cancerous cells, as previously reported [21]. This low baseline expression suggests that DEK upregulation is tightly associated with pathological states, reinforcing its context-dependent role as either an oncogene or a compensatory regulator in abnormal cellular environments.

Although our study did not identify statistically significant differences in DEK gene expression across normal, benign, and malignant gynecological tissues, significant variations in DEK protein expression patterns were observed. These findings suggest DEK as a potential biomarker for early screening, particularly in Pap smears, to detect DNA damage or early tumorigenic changes. Monitoring DEK protein levels could enable early detection of genetic instability associated with fibroids and cervical cancer, offering opportunities for timely intervention and improved outcomes. Incorporating DEK into screening protocols, as suggested in other cancers [39–41], could address a critical need in women's health. However, as a pilot study with a limited sample size, further research is needed to validate these results and assess DEK mRNA expression differences across tissue types to solidify its biomarker potential.

These findings also underscore the necessity for further elucidation of the molecular mechanisms underlying DEK's role in gynecological tumorigenesis, particularly its crosstalk with key oncogenic pathways, including p53, TGF-β, and sphingosine-1-phosphate (S1P). DEK's capacity to stabilize p53 and TGF-β receptors and modulate downstream signaling cascades is of significant interest, given TGF-β's

pivotal involvement in cellular proliferation, differentiation, apoptosis, motility, and angiogenesis, as well as the frequent inactivation of p53 in nearly 50% of malignancies and S1P's critical role in tumor angiogenesis and microenvironmental regulation [50–54]. The hormonal regulation of DEK also warrants exploration, particularly its differential expression in benign versus malignant gynecological tissues. Estrogen, progesterone, and androgen have been identified as modulators of DEK expression through hormone-specific signaling axes; for instance, estrogen directly promotes DEK transcription via nuclear receptor binding, while progesterone receptor isoform B levels in uterine myomas positively correlate with tumor burden and inversely with symptom severity, including intermenstrual bleeding and dysmenorrhea [4, 55]. Investigating DEK's expression dynamics across the menstrual cycle, as well as its stability in postmenopausal tissues devoid of hormonal fluctuations, could delineate its endocrine dependence and functional relevance in hormone-driven tumorigenesis. Moreover, tissue-specific interrogation of DEK expression between cervical cancer samples and unaffected myometrial tissues may clarify whether its oncogenic role is confined to the cervix or extends across uterine compartments. Such comparative analyses could provide mechanistic insights into DEK's involvement in tumor biology, its modulation of the local microenvironment, and its tissue-specific contributions to oncogenic progression.

CONCLUSION

In conclusion, the significant upregulation of DEK in cervical cancer, its intermediate expression in uterine myomas, and negligible levels in normal tissues highlight its role in tumor progression and its potential as a biomarker for early detection, warranting further investigation to improve gynecological cancer management and address a crucial need in women's health.

Declaration of generative AI and AI-assisted technologies in the writing process

During the preparation of this work the authors used ChatGPT in order to improve the readability and language of the manuscript. After using this tool, the authors reviewed and edited the content as needed and take full responsibility for the content of the publication.

Funding statement

Conflict of interest

None to report.

REFERENCES

1. Pruksananonda K, Wasinarom A, Mutirangura A. Epigenetics in human reproduction and gynecologic diseases. *Epigenetics Hum Dis.* 2024:959-86.

2. Weiderpass E, Labrèche F. Malignant tumors of the female reproductive system. *Saf Health Work.* 2012;3(3):166-80.

3. Tsigkou A, et al. Expression levels of myostatin and matrix metalloproteinase 14 mRNAs in uterine leiomyoma are correlated with dysmenorrhea. *Reprod Sci.* 2015;22(12):1597-602.

4. Tsigkou A, et al. Increased progesterone receptor expression in uterine leiomyoma: correlation with age, number of leiomyomas, and clinical symptoms. *Fertil Steril.* 2015;104(1):170-5.

5. Kim JJ, Sefton EC. The role of progesterone signaling in the pathogenesis of uterine leiomyoma. *Mol Cell Endocrinol.* 2012;358(2):223-31.

6. Cohen PA, et al. Cervical cancer. *Lancet.* 2019;393(10167):169-82.

7. National Cancer Institute. Cervical cancer screening. 2022.

8. Boone JD, Erickson BK, Huh WK. New insights into cervical cancer screening. *J Gynecol Oncol.* 2012;23(4):282.

9. Spence AR, Goggin P, Franco EL. Process of care failures in invasive cervical cancer: systematic review and meta-analysis. *Prev Med.* 2007;45(2-3):93-106.

10. Cuzick J, et al. Overview of the European and North American studies on HPV testing in primary cervical cancer screening. *Int J Cancer.* 2006;119(5):1095-101.

11. Testa AC, et al. Imaging techniques for evaluation of uterine myomas. *Best Pract Res Clin Obstet Gynaecol.* 2016;34:37-53.

12. Khan AT, Shehmar M, Gupta JK. Uterine fibroids: current perspectives. *Int J Women's Health.* 2014:95-114.

13. Wilde S, Scott-Barrett S. Radiological appearances of uterine fibroids. *Indian J Radiol Imaging.* 2009;19(03):222-31.

14. Killeen JL, et al. Improved abnormal Pap smear triage using cervical cancer biomarkers. *J Low Genit Tract Dis.* 2014;18(1):1-7.

15. Mäkinen N, et al. Characterization of MED12, HMGA2, and FH alterations reveals molecular variability in uterine smooth muscle tumors. *Mol Cancer.* 2017;16:1-8.

16. Hersch J, et al. Psychosocial interventions and

quality of life in gynaecological cancer patients: a systematic review. *Psycho-Oncology: J Psychol., Soc Behav Dimens Cancer.* 2009;18(8):795-810.

17. Sung H, et al. Global cancer statistics 2020: GLOBOCAN estimates of incidence and mortality worldwide for 36 cancers in 185 countries. CA: a cancer journal for clinicians. 2021;71(3):209-49.

18. Pilié PG, et al. State-of-the-art strategies for targeting the DNA damage response in cancer. *Nat Rev Clin Oncol.* 2019 ;16(2):81-104.

19. Adam ML, et al. Assessment of the association between micronuclei and the degree of uterine lesions and viral load in women with human papillomavirus. *Cancer Genom Proteom.* 2015;12(2):67-71.

20. Liu K, et al. Silencing of the DEK gene induces apoptosis and senescence in CaSki cervical carcinoma cells via the up-regulation of NF-κB p65. *Biosci. Rep.* 2012;32(3):323-32.

21. Riveiro-Falkenbach E, Soengas MS. Control of tumorigenesis and chemoresistance by the DEK oncogene. *Clin Cancer Res.* 2010;16(11):2932-8.

22. Kavanaugh GM, et al. The human DEK oncogene regulates DNA damage response signaling and repair. *Nucleic Acids Res.* 2011;39(17):7465-76.

23. Sammons M, et al. Negative regulation of the RelA/p65 transactivation function by the product of the DEK proto-oncogene. *J Biol Chem.* 2006;281(37):26802-12.

24. McGarvey T, et al. The acute myeloid leukemia-associated protein, DEK, forms a splicing-dependent interaction with exon-product complexes. *J Cell Biol.* 2000;150(2):309-20.

25. Vassilios Alexiadis, et al. The protein encoded by the proto-oncogene DEK changes the topology of chromatin and reduces the efficiency of DNA replication in a chromatin-specific manner. *Genes Dev.* 2000 ;14(11):1308–12.

26. Yu L, et al. Critical role of DEK and its regulation in tumorigenesis and metastasis of hepatocellular carcinoma. *Oncotarget.* 2016;7(18):26844.

27. Kappes F, et al. Subcellular localization of the human proto-oncogene protein DEK. *J Biol Chem.* 2001;276(28):26317-23.

28. Yang MQ, et al. DEK promotes the proliferation and invasion of lung cancers and indicates poor prognosis in lung adenocarcinomas. *Oncol Rep.* 2020;43(4):1338-48.

29. Privette Vinnedge LM, et al. The human DEK oncogene stimulates β-catenin signaling, invasion and mammosphere formation in breast cancer. *Oncogene.* 2011;30(24):2741-52.

30. Liu B, et al. DEK modulates both expression and alternative splicing of cancer-related genes. *Oncol Rep.* 2022;47(6):1-4.

31. Hacker KE, et al. The DEK oncoprotein functions in ovarian cancer growth and survival. *Neoplasia.* 2018;20(12):1209-18.

32. Liu K, et al. Silencing of the DEK gene induces apoptosis and senescence in CaSki cervical carcinoma cells via the up-regulation of NF-κB p65. *Biosci Rep.* 2012;32(3):323-32.

33. Xu X, Zou L, et al. Silencing DEK downregulates cervical cancer tumorigenesis and metastasis via the DEK/p-Ser9-GSK-3β/p-Tyr216-GSK-3β/β-catenin axis. *Oncol Rep.* 2017;38(2):1035-42.

34. Anderson MW, et al. Role of proto-oncogene activation in carcinogenesis. *Environ Health Perspect.* 1992;98:13-24.

35. TORRY DS, COOPER GM. Proto-Oncogenes in Development and Cancer. *Am J Reprod Immunol.* 1991;25(3):129-32.

36. Feng K, et al. Emerging proteins involved in castration-resistant prostate cancer via the AR-dependent and AR-independent pathways. *Int J Oncol.* 2023 ;63(5):1-7.

37. Han S, et al. Clinicopathological significance of DEK overexpression in serous ovarian tumors. *Pathol Int.* 2009 ;59(7):443-7.

38. Privette Vinnedge LM, et al. The DEK oncogene promotes cellular proliferation through paracrine Wnt signaling in Ron receptor-positive breast cancers. *Oncogene.* 2015;34(18):2325-36.

39. Wise-Draper TM, et al. Overexpression of the cellular DEK protein promotes epithelial transformation in vitro and in vivo. *Cancer Res.* 2009;69(5):1792-9.

40. Riveiro-Falkenbach E, et al. DEK oncogene is overexpressed during melanoma progression. *Pigment Cell Melanoma Res.* 2017;30(2):194-202.

41. Kappes F, et al. DEK expression in melanocytic lesions. *Hum Pathol.* 2011;42(7):932-8.

42. Wise-Draper TM, et al. Apoptosis inhibition by the

human DEK oncoprotein involves interference with p53 functions. *Mol Cell Biol*. 2006; 26(20) 7506-09.

43. Burmeister CA, et al. Cervical cancer therapies: Current challenges and future perspectives. *Tumour Virus Res*. 2022;13:200238.

44. Wu Q, et al. DEK overexpression in uterine cervical cancers. *Pathol Int*. 2008;58(6):378-82.

45. Yang MQ, et al. DEK is highly expressed in breast cancer and is associated with malignant phenotype and progression. *Oncol Lett*. 2021;21(6):1-9.

46. Lee KF, et al. DEK is a potential biomarker associated with malignant phenotype in gastric cancer tissues and plasma. *Int J Mol Sci*. 2019;20(22):5689.

47. Deutzmann A, et al. The human oncoprotein and chromatin architectural factor DEK counteracts DNA replication stress. *Oncogene*. 2015;34(32):4270-7.

48. Habiburrahman M, et al. Potential of DEK proto-oncogene as a prognostic biomarker for colorectal cancer: An evidence-based review. *Mol Clin Oncol*. 2022;17(1):1-0.

49. Yang MQ, et al. DEK is highly expressed in breast cancer and is associated with malignant phenotype and progression. *Oncol Lett*. 2021;21(6):1-9.

50. Wise-Draper TM, et al. Apoptosis inhibition by the human DEK oncoprotein involves interference with p53 functions. *Mol Cell Biol*. 2006;26(20)7506-19.

51. Song Y, et al. DEK-targeting aptamer DTA-64 attenuates bronchial EMT-mediated airway remodelling by suppressing TGF-β1/Smad, MAPK and PI3K signalling pathway in asthma. *J Cell Mol Med*. 2020;24(23):13739-50.

52. Shepherd JH. Revised FIGO staging for gynaecological cancer. *BJOG: Int J Obstet Gynaecol*. 1989;96(8):889-92.

53. Zhang C, et al. Gain-of-function mutant p53 in cancer progression and therapy. *J Mol Cell Biol*. 2020;12(9):674-87.

54. Du W, et al. S1P2, the G protein–coupled receptor for sphingosine-1-phosphate, negatively regulates tumor angiogenesis and tumor growth in vivo in mice. *Cancer Res*. 2010;70(2):772-81.

55. Privette Vinnedge LM, et al. The DEK oncogene is a target of steroid hormone receptor signaling in breast cancer.

56. Yang Y, et al. DEK promoted EMT and angiogenesis through regulating PI3K/AKT/mTOR pathway in triple-negative breast cancer. *Oncotarget*. 2017;8(58):98708.